Biochimica et Biophysica Acta 1850 (2015) 824–831

Contents lists available at ScienceDirect

Biochimica et Biophysica Acta

journal homepage: www.elsevier.com/locate/bbagen

Andrographolide ameliorates diabetic retinopathy by inhibiting retinal angiogenesis and inflammation

Zengyang Yu [a], Bin Lu [a], Yuchen Sheng [b], Lingyu Zhou [a], Lili Ji [a,*], Zhengtao Wang [a]

[a] The Shanghai Key Laboratory of Complex Prescription and MOE Key Laboratory for Standardization of Chinese Medicines, Institute of Chinese Materia Medica, Shanghai University of Traditional Chinese Medicine, Shanghai 201203, China
[b] Center for Drug Safety Evaluation and Research, Shanghai University of Traditional Chinese Medicine, Shanghai 201203, China

ARTICLE INFO

Article history:
Received 6 November 2014
Received in revised form 12 January 2015
Accepted 20 January 2015
Available online 29 January 2015

Keywords:
Andrographolide
Diabetic retinopathy
Angiogenesis
Inflammation

ABSTRACT

Background: Andrographolide (Andro) is the main compound distributed in medicinal herb *Andrographis paniculata*. This study aims to observe the amelioration of Andro on streptozotocin (STZ)-induced diabetic retinopathy (DR) in mice.
Methods: STZ-induced non-proliferative DR (NPDR) for 2 months and proliferative DR (PDR) for 5 month in C57BL/6 mice were used in this study, respectively. Retinal vessels were observed by immunofluorescence staining for cluster of differentiation 31 (CD31). Evans blue permeation assay was used to detect the breakdown of blood-retinal barrier (BRB). Real-time PCR and immune-blot were used to detect mRNA and protein expression. Enzyme-linked immunosorbent assay (ELISA) was used to detect serum tumor necrosis factor-α (TNF-α), interleukin (IL)-6, and IL-1β.
Results: Retinal immunofluorescence staining with CD31 showed that Andro reduced the increased retinal vessels in STZ-induced PDR mice. Evans blue permeation results demonstrated that Andro attenuated the breakdown of BRB in STZ-induced NPDR mice. In STZ-induced PDR mice, Andro decreased the increased vascular endothelial growth factor (VEGF) in serum and vitreous cavity, and reduced the increased retinal mRNA expression of VEGF and its receptors. In STZ-induced NPDR mice, Andro abrogated the nuclear translocation of nuclear factor κB (NF-κB) p65 and early growth response-1 (Egr-1), and reduced the increased phospho-NF-κBp65, -inhibitor of kappa B (IκB), and -IκB kinase (IKK). Andro also decreased the increased serum and retinal mRNA expression of TNF-α, IL-6, IL-1β, serpine1, and tissue factor (TF).
Conclusions: Andro ameliorates DR via attenuating retinal angiogenesis and inflammation, and VEGF, NF-κB, and Egr1 signaling pathways all play important roles in this process.

1. Introduction

With the changing of lifestyle and the increasing of aging population, diabetes mellitus (DM) has been a serious and concerning health problem in the world. In China, the number of people who suffered from diabetes is about 98.4 million in the year 2013, which is the highest in the world [1]. DM is generally associated with severe complications such as diabetic retinopathy (DR) and diabetic nephropathy, which greatly reduce the quality of life and the survival of diabetic patients. DR, the chronic vascular complication due to the development of DM, is one of the most common and serious complications of DM [2,3]. Vision loss from DR has been a major and leading cause of blindness in adult. It is reported that nearly all persons with type 1 diabetes and about 60% of persons with type 2 diabetes will develop DR when living with DM for the first two decades [4,5].

The classification of DR mainly includes non-proliferative DR (NPDR) and proliferative DR (PDR) according to the International Clinical Diabetic Retinopathy Disease Severity Scale [6]. NPDR is characterized by selective loss of pericytes, the formation of acellular capillaries, the thickening of basement membrane, the increased vascular permeability, and capillary occlusion [5,7]. The resulting ischemia due to capillary non-perfusion leads to the increased secretion of various growth factors including VEGF, which promotes neoangiogenesis in retina, and retinal angiogenesis is the hallmark of PDR [5,7]. Thus, anti-inflammation and anti-angiogenesis have been considered as the potential therapeutic strategies for DR [8].

Abbreviations: Andro, Andrographolide; DR, diabetic retinopathy; STZ, streptozotocin; NPDR, non-proliferative DR; PDR, proliferative DR; CD31, cluster of differentiation 31; BRB, blood-retinal barrier; VEGF, vascular endothelial growth factor; ELISA, enzyme-linked immunosorbent assay; TNF-α, tumor necrosis factor-α; IL, interleukin; NF-κB, nuclear factor κB; Egr-1, early growth response-1; IκB, inhibitor of kappa B; IKK, IκB kinase; TF, tissue factor; DM, diabetes mellitus; FITC, fluorescein isothiocyanate; HMGB1, high-mobility group box-1; RAGE, receptor for advanced glycation end products; OPN, osteopontin; tPA, tissue plasminogen

* Corresponding author at: The Shanghai Key Laboratory of Complex Prescription and MOE Key Laboratory for Standardization of Chinese Medicines, Institute of Chinese Materia Medica, Shanghai University of Traditional Chinese Medicine, 1200 Cailun Road, Shanghai 201203, China. Tel.: +86 21 51322517; fax: +86 21 51322505.
E-mail address: lichenyue1307@126.com (L. Ji).

http://dx.doi.org/10.1016/j.bbagen.2015.01.014
0304-4165/

Table 1
Sequences of primers used for real-time RT-PCR.

Target	Primer	Sequence annealing temperature (°C)
Actin	FP	5′-TTCGTTGCCGGTCCACACCC-3′ 61 °C
	RP	5′-GCTTTGCACATGCCGGAGCC-3′
VEGFA	FP	5′-GCTACTGCCGTCCGATTGAG-3′ 60 °C
	RP	5′-ACTCCAGGGCTTCATCGTTACAG-3′
FLT-1	FP	5′-CCTGATGGGCAAAGAATAACAT-3′ 60 °C
	RP	5′-ATTTGGACATCTAGGATTGTATTGG-3′
KDR	FP	5′-GTGGTAAGTTGCGATTGTTGTG-3′ 60 °C
	RP	5′-TGAACATTCGCCTTCTTTGATA-3′
IL-1β	FP	5′-AAAAAAGCCTCGTGCTGTCG-3′ 60 °C
	RP	5′-GTCGTTGCTTGGTTCTCCTTG-3′
IL-6	FP	5′-ACAAAGCCAGAGTCCTTCAGAGAG-3′ 62 °C
	RP	5′-TTGGATGGTCTTGGTCCTTAGCC-3′
TNFa	FP	5′-CTGAACTTCGGGGTGATCGGT-3′ 62 °C
	RP	5′-TCCTCCACTTGGTGGTTTGCTAC-3′
Egr-1	FP	5′-GGCGATGGTGGAGACGAGTTAT-3′ 58 °C
	RP	5′-CAAAGTGTTGCCACTGTTGGGT-3′
TF	FP	5′-ACACAAACCTTGGACAGCCAGTAA-3′ 59 °C
	RP	5′-CTTTCCCGTGCTTGAGCCTTT-3′
Serpine1	FP	5′-ACAGCTCATGCCCTCCGCCA-3′ 62 °C
	RP	5′-CACCAGGCGTGTCAGCTCGTC-3′

Andrographolide (Andro), a natural diterpenoid lactone, is the main compound isolated from traditional medicinal herb *Andrographis paniculata* Nees (Acanthaceae) [9]. *A. paniculata* Nees is well-known for clearing away heat and toxic materials, and has been widely used for centuries in Asian countries like China, India, and Thailand for the treatment of sore throat, flu and upper respiratory tract infections [9]. There are various reports about the anti-inflammatory activity of andrographolide in experimental models of asthma, cigarette smoke-induced lung injury, pulmonary fibrosis, inflammatory bowel disease, etc. [10–13]. In addition, andrographolide is also reported to inhibit tumor angiogenesis in vivo and in vitro [14–16]. As andrographolide has obvious anti-inflammatory and anti-angiogenic activity, it may have potential therapeutic activity against DR. The present study aims to observe the amelioration of andrographolide on DR (including NPDR and PDR), and further explore the engaged mechanisms from inhibiting retinal inflammation and angiogenesis.

2. Materials and methods

2.1. Chemical compounds and reagents

Andrographolide (Andro), its purity is above 98.5%, was purchased from Nanjing TCM Institute of Chinese Materia Medica (Nanjing, China). Cluster of differentiation 31 (CD31) antibody and fluorescein isothiocyanate (FITC) conjugated anti-Rat IgG were purchased from BD Biosciences (Franklin Lakes, NJ). Enzyme-linked immunosorbent assay (ELISA) kit for VEGF was obtained from R&D (Minneapolis, MN), and other ELISA kits were purchased from RapidBio (West Hills, CA). Trizol reagent was purchased from Life Technology (Carlsbad, CA). PrimeScript® RT Master Mix and SYBR® Premix Ex Taq™ were purchased from Takara (Shiga, Japan). NE-PER® nuclear and cytoplasmic extraction reagents and Pierce® BCA Protein Assay Kit were purchased from Thermo Scientific (Bremen, Germany). NF-κBp65, phospho-NF-κBp65, phospho-IκB, phospho-IKK, Egr1, β-actin, and LaminB antibodies were all purchased from Cell Signaling Technology (Danvers, MA). Peroxidase-conjugated goat anti-Rabbit IgG (H + L) and peroxidase-conjugated goat anti-Mouse IgG (H + L) were purchased from Jackson ImmunoResearch (West Grove, PA). Other reagents unless indicated were purchased from Sigma Chemical Co. (St. Louis, MO).

2.2. Experimental animals

The C57BL/6 mice (18–22 g) were purchased from the Shanghai Laboratory Animal Center of Chinese Academy of Sciences (Shanghai, China). The animals were maintained under controlled temperature (23 ± 2 °C), humidity (50%), and lighting (12 h light/12 h dark). The animals were fed with a standard laboratory diet and given free access to tap water. All animals received humane care according to the institutional animal care guidelines approved by the Experimental Animal Ethical Committee of Shanghai University of Traditional Chinese Medicine.

2.3. Establishment of the mice model of STZ-induced NPDR

Thirty-five mice were administered intraperitoneally (i.p.) with 55 mg/kg STZ for 5 consecutive days, while the other sixteen mice were injected (i.p.) with physiological saline and served as control animals. The concentration of serum glucose was measured 7 days after the last injection, and the mice with high glucose concentration (>16.5 mmol/L) were considered as diabetic mice. In this experiment, the glucose concentration of 33 mice was >16.5 mmol/L, and those mice were randomly divided into two groups: NPDR model (n = 17) and NPDR + Andro (10 mg/kg) (n = 16), respectively. At 1 month after the injection of STZ, the mice were administered intraperitoneally (i.p.) with Andro (10 mg/kg per day) consecutively for 1 month. At 2 months after the injection of STZ, 6 mice of each group were used for the measurement of BRB breakdown by using Evans blue. The other mice were anesthetized by sodium pentobarbital (30 mg/kg, i.p.), the blood samples were taken from the abdominal aorta, and the eyes were removed immediately.

2.4. Establishment of the mice model of STZ-induced PDR

Twenty-two mice were administered intraperitoneally (i.p.) with 55 mg/kg STZ for 5 consecutive days, while the other ten mice were injected (i.p.) with physiological saline and served as control animals. The concentration of serum glucose was measured 7 days after the

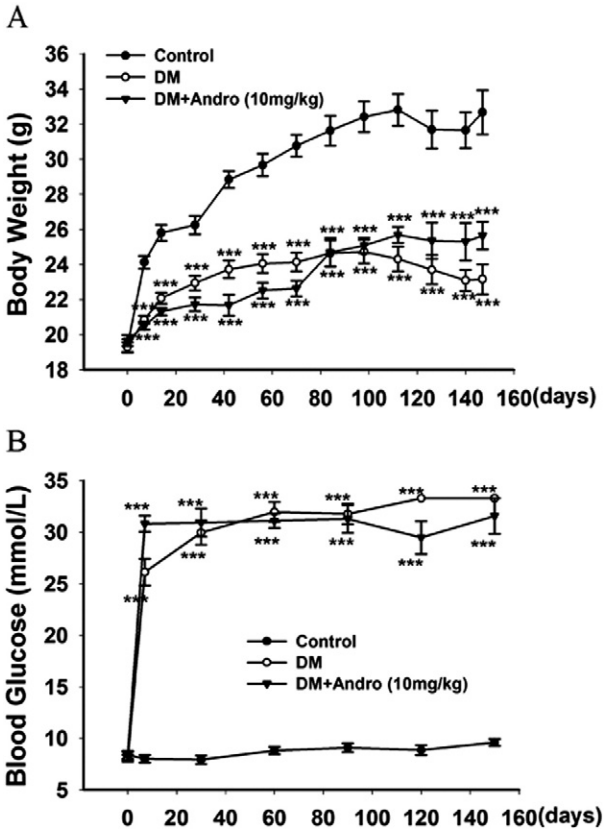

Fig. 1. Analysis of body weight and blood glucose level. (A) Body weight; (B) blood glucose level. Data = Means ± SEM (n = 9 for control, n = 10 for DM, n = 8 for Andro). ***$P < 0.001$ compared to control.

last injection, and the mice with high glucose concentration (>16.5 mmol/L) were considered as diabetic mice. In this experiment, the glucose concentration of 19 mice was >16.5 mmol/L, and those mice were randomly divided into two groups: PDR model (n = 10) and PDR + Andro (10 mg/kg) (n = 9), respectively. At 3 months after the injection of STZ, the mice were administered intraperitoneally (i.p.) with Andro (10 mg/kg per day) consecutively for 2 months. At 5 months after the injection of STZ, the mice were anesthetized by sodium pentobarbital (30 mg/kg, i.p.), the blood samples were taken from the abdominal aorta, and the eyes were removed immediately. Meanwhile, the body weight was monitored and the concentration of blood glucose was determined by Glucometer® (Accu-Check® Performa Nano, Roche Diagnostics, Germany) during the whole experimental process.

2.5. Retinal cluster of differentiation 31 (CD31) immunofluorescence staining

The experimental procedure of retinal CD31 immunofluorescence staining was described in our previous published papers [17,18], and the retinas were pictured under the fluorescence microscopy (IX81, Olympus, Japan). The quantity of the vessels was counted as in previously described method [17–19].

2.6. Measurement of blood-retinal barrier (BRB) breakdown using Evans blue

Mice were injected with 2% Evans blue (10 μl/g, i.p.) in PBS. After 2 h, blood was extracted through the left ventricle; and the mice were perfused with PBS to completely remove the Evans blue dye in blood vessels. Retinas were carefully dissected and the weight was determined after thoroughly drying. Next, the retinas were incubated in 120 μl formamide for 18 h at 70 °C to extract the Evans blue dye. The extract was centrifuged at 10,000 *g* twice for 1 h at 4 °C. Absorbance of the supernatant was measured with a spectrophotometer at 620 nm. The concentration of Evans blue dye in extracts was calculated using a standard curve of Evans blue in formamide and normalized to the dried retinal weight.

2.7. ELISA analysis

The whole blood and fluids in vitreous cavity were centrifuged at 3000 rpm, 4 °C for 15 min, and serum and fluids in vitreous cavity were collected for ELISA analysis according to the manufacturer's instructions.

2.8. RNA isolation and cDNA synthesis

Total RNA in retinas was isolated using Trizol reagent according to the instruction. The RNA content was determined by measuring the optical density at 260 nm, and cDNA was synthesized according to the instruction described in the kits.

2.9. Real-time PCR analysis

Real-time PCR was performed using a SYBR green premix according to the instruction. Relative expression of target genes was normalized to Actin, analyzed by $2^{-\Delta\Delta Ct}$ method and given as ratio compared with the control. The primer sequences used in this study are shown in Table 1.

2.10. Nuclear and cytoplasm protein extraction

Retinal cytosolic and nuclear proteins were isolated as described in NE-PER® nuclear and cytoplasmic extraction kits. The protein

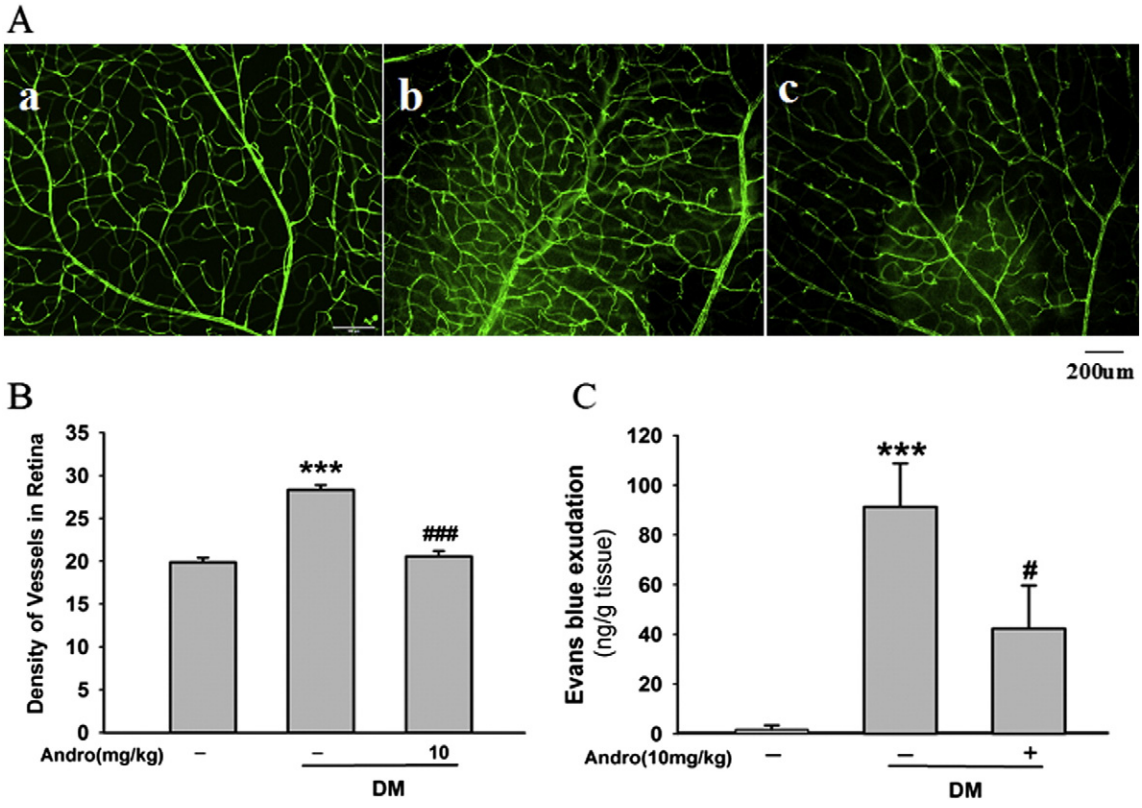

Fig. 2. Andro inhibited retinal angiogenesis in STZ-induced PDR mice and attenuated BRB breakdown in STZ-induced NPDR mice. (A) Immunofluorescence staining of retinas with CD31 in STZ-induced PDR mice, and the enlarged partial view of CD31-stained retina was showed (original magnification ×100). (a. Control, b. DM, c. DM + Andro 10 mg/kg). (B) Quantitative results of CD31-stained retinal vessels. Data = Means ± SEM (n = 4). $^{***}P < 0.001$ compared to control; $^{\#\#\#}P < 0.001$ compared to DM without Andro. (C) BRB breakdown was detected by using Evans blue leakage assay in STZ-induced NPDR mice. Data = Means ± SEM (n = 6). $^{***}P < 0.001$ compared to control; $^{\#}P < 0.05$ compared to DM without Andro.

concentration of samples was detected by Pierce® BCA Protein Assay Kit, and all the samples were normalized to the equal protein concentration.

2.11. Western-blot analysis

Retinas were homogenized in ice-cold lysis buffer containing 50 mM Tris, pH 7.5, 150 mM NaCl, 1 mM EDTA, 20 mM NaF, 0.5% NP-40, 10% glycerol, 1 mM phenylmethylsulfonyl fluoride 10 μg/ml aprotinin, 10 μg/ml leupeptin, and 10 μg/ml pepstatin A. After centrifugation, protein concentration of the resulting supernatant was determined, and normalized to equal amount of protein of each sample. Proteins were separated by SDS-PAGE and blots were probed with appropriate combination of primary and horseradish peroxidase-conjugated secondary antibodies. Proteins were visualized by enhanced chemiluminescence kits. For repeated immunoblotting, membranes were stripped in 62.5 mM Tris (pH 6.7), 20% SDS and 0.1 M 2-mercaptoethanol for 30 min at 50 °C.

2.12. Statistical analysis

Data were expressed as means ± standard error of the mean. The significance of differences between groups was evaluated by one-way ANOVA with LSD post hoc test, and $P < 0.05$ was considered as statistically significant differences.

3. Results

3.1. Measurement of body weight and blood glucose concentration

As shown in Fig. 1A, the body weight of diabetic mice was obviously lower than that of normal control mice ($P < 0.001$), and there was weak amelioration of body weight after the treatment of Andro (10 mg/kg). Further, Fig. 1B showed that blood glucose concentration in dibetic mice was obviously higher than that in normal control mice ($P < 0.001$), while after Andro (10 mg/kg) treatment there was not much effect on the elevated blood glucose concentration in diabetic mice.

3.2. Andro inhibited retinal angiogenesis in STZ-induced PDR mice

The inhibition of Andro on retinal angiogenesis in STZ-induced PDR mice was observed by staining retinal vessels using CD31. Fig. 2A is the partially enlarged picture of CD31-stained retinas. From Fig. 2A, we can see that there were more CD31-stained vessels in diabetic mice (Fig. 2A-b) than in normal control mice (Fig. 2A-a), whereas such increased vessels were diminished in diabetic mice after treated with Andro (10 mg/kg) (Fig. 2A-c). Further, after counting the number of vessels, we can see that Andro (10 mg/kg) obviously decreased the increased number of retinal vessels in diabetic mice ($P < 0.001$) (Fig. 2B).

3.3. Andro attenuated BRB breakdown in STZ-induced NPDR mice

The attenuation of Andro on BRB breakdown in STZ-induced NPDR mice was observed by using Evans blue leakage assay. As shown in Fig. 2C, the results of Evans blue leakage assay showed that there was increased vessel leakage in STZ-induced diabetic mice ($P < 0.001$), whereas Andro (10 mg/kg) obviously inhibited such increased vessel leakage in STZ-induced diabetic mice ($P < 0.05$).

3.4. Effects of Andro on VEGF expression in STZ-induced PDR mice

Further, the effects of Andro on the expression of VEGF, which is the main growth factor for stimulating angiogenesis, were observed in STZ-induced PDR mice. As shown in Fig. 3A, Andro (10 mg/kg) decreased the elevated serum VEGF content in STZ-induced diabetic mice ($P < 0.01$). In addition, Andro (10 mg/kg) also decreased the

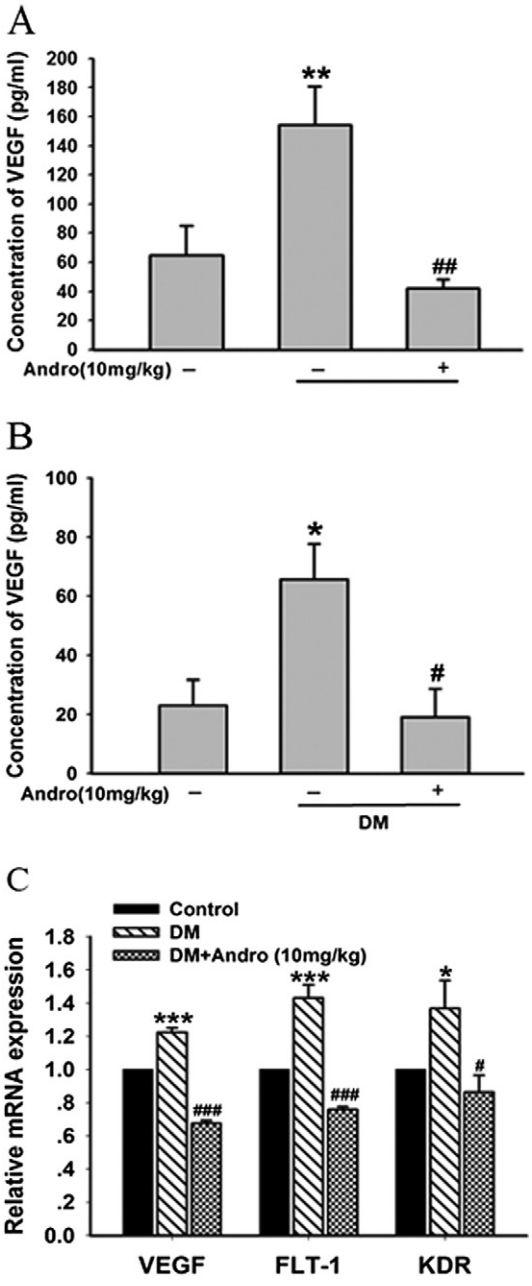

Fig. 3. Effects of Andro on VEGF expression in STZ-induced PDR mice. (A) Serum content of VEGF. Data = Means ± SEM (n = 6). (B) VEGF content in vitreous cavity. Data = Means ± SEM (n = 8 for control, n = 8 for DM, n = 6 for Andro). (C) Retinal mRNA expression of VEGF and its receptors including FLT-1 and KDR. Data = Means ± SEM (n = 7 for control, n = 8 for DM, n = 6 for Andro). $^{*}P < 0.05$, $^{**}P < 0.01$, $^{***}P < 0.001$ compared to control; $^{\#}P < 0.05$, $^{\#\#}P < 0.01$, $^{\#\#\#}P < 0.001$ compared to DM without Andro.

increased VEGF content in vitreous cavity in diabetic mice ($P < 0.05$) (Fig. 3B). Further, the results of real-time PCR analysis showed that Andro (10 mg/kg) decreased the elevated mRNA expression of VEGF and its receptors like FLT-1 and KDR in retinas in STZ-induced diabetic mice ($P < 0.05$, $P < 0.001$).

3.5. Effects of Andro on NF-κB signaling pathway in STZ-induced NPDR mice

As shown in Fig. 4A, we can see that Andro (10 mg/kg) obviously decreased the increased expression of NFκBp65 in retinal nucleus in diabetic mice. After calculating the gray density of the protein bands (Fig. 4B), the expression of NF-κBp65 was obviously increased in retinal nucleus in STZ-induced diabetic mice ($P < 0.001$), but not changed in

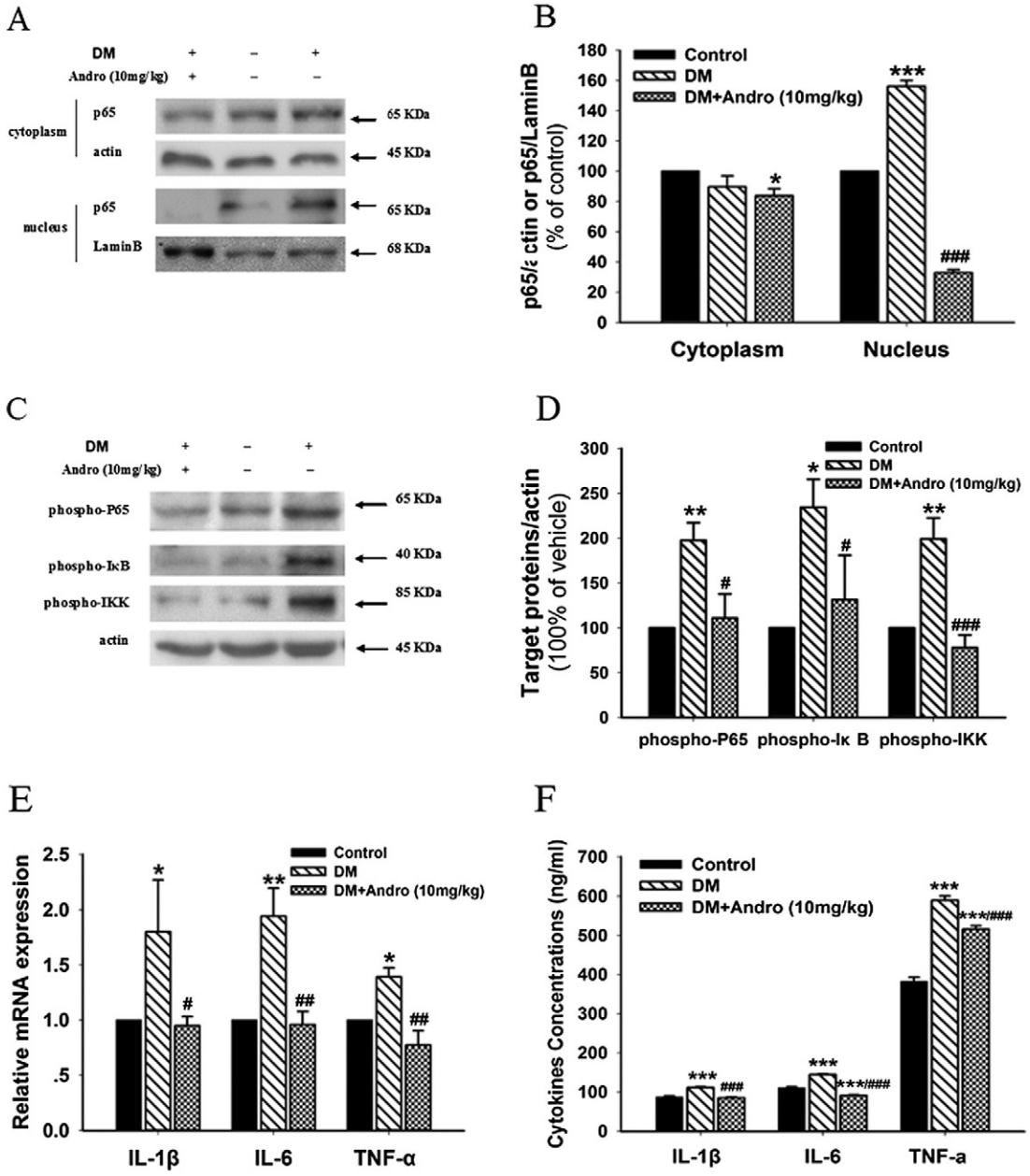

Fig. 4. Effect of Andro on NF-κB signaling pathway in STZ-induced NPDR mice. (A) Andro inhibited the nuclear translocation of NF-κBp65 protein in retinas. Results represent at least three repeated experiments. (B) Quantitative densitometric analysis of NF-κBp65 in cytoplasm and nucleus. (C) Retinal expression of phosphorylated NF-κBp65, IκB, IKK. Phosphorylated NF-κBp65, IκB, IKK are detected by immunoblotting using specific antibodies. Results represent at least three repeated experiments. (D) Quantitative densitometric analysis of phosphorylated NF-κBp65, IκB, IKK. (E) Retinal mRNA expression of TNF-α, IL-1β, IL-6. (F) Serum contents of TNF-α, IL-1β, IL-6. Data are expressed as means ± SEM (n = 9 for control, n = 11 for DM, n = 10 for Andro). $^{*}P < 0.05$, $^{**}P < 0.01$, $^{***}P < 0.001$ compared to control; $^{\#}P < 0.05$, $^{\#\#}P < 0.01$, $^{\#\#\#}P < 0.001$ compared to DM without Andro.

retinal cytoplasm. After mice were treated with Andro (10 mg/kg), the increased retinal nuclear NF-κBp65 was obviously decreased in diabetic mice ($P < 0.001$). Meanwhile, Andro (10 mg/kg) also weakly decreased the expression of NF-κBp65 in retinal cytoplasm in diabetic mice ($P < 0.05$).

Further results in Fig. 4C demonstrated that the expression of phosphorylated NF-κBp65, IκB and IKK proteins was obviously increased in retinas of STZ-induced diabetic mice, whereas Andro (10 mg/kg) decreased such elevated expression of phospho-NF-κBp65, -IκB and -IKK. The inhibition of Andro on the phosphorylated activation of NF-κBp65, IκB and IKK proteins was confirmed in the results of gray density of protein bands in Fig. 4D ($P < 0.05$, $P < 0.001$).

As shown in Fig. 4E, retinal mRNA expression of IL-1β, IL-6, and TNF-α was increased in STZ-induced diabetic mice ($P < 0.05$, $P < 0.01$), whereas such increased mRNA expression was reduced in Andro-treated diabetic mice ($P < 0.05$, $P < 0.01$). In addition, the results of Fig. 4F showed that serum levels of IL-1β, IL-6, and TNF-α were increased in STZ-induced diabetic mice ($P < 0.05$, $P < 0.01$). After mice were treated with Andro (10 mg/kg), the elevated serum levels of IL-1β, IL-6, and TNF-α were all decreased ($P < 0.05$, $P < 0.01$).

3.6. Effects of Andro on Egr1 signaling pathway in STZ-induced NPDR mice

As shown in Fig. 5A, we can see that Andro (10 mg/kg) obviously decreased the increased expression of Egr1 in retinal nucleus in STZ-induced diabetic mice. After calculating the gray density of the protein bands (Fig. 5B), the expression of Egr1 was obviously increased in retinal nucleus in STZ-induced diabetic mice ($P < 0.05$). After mice were

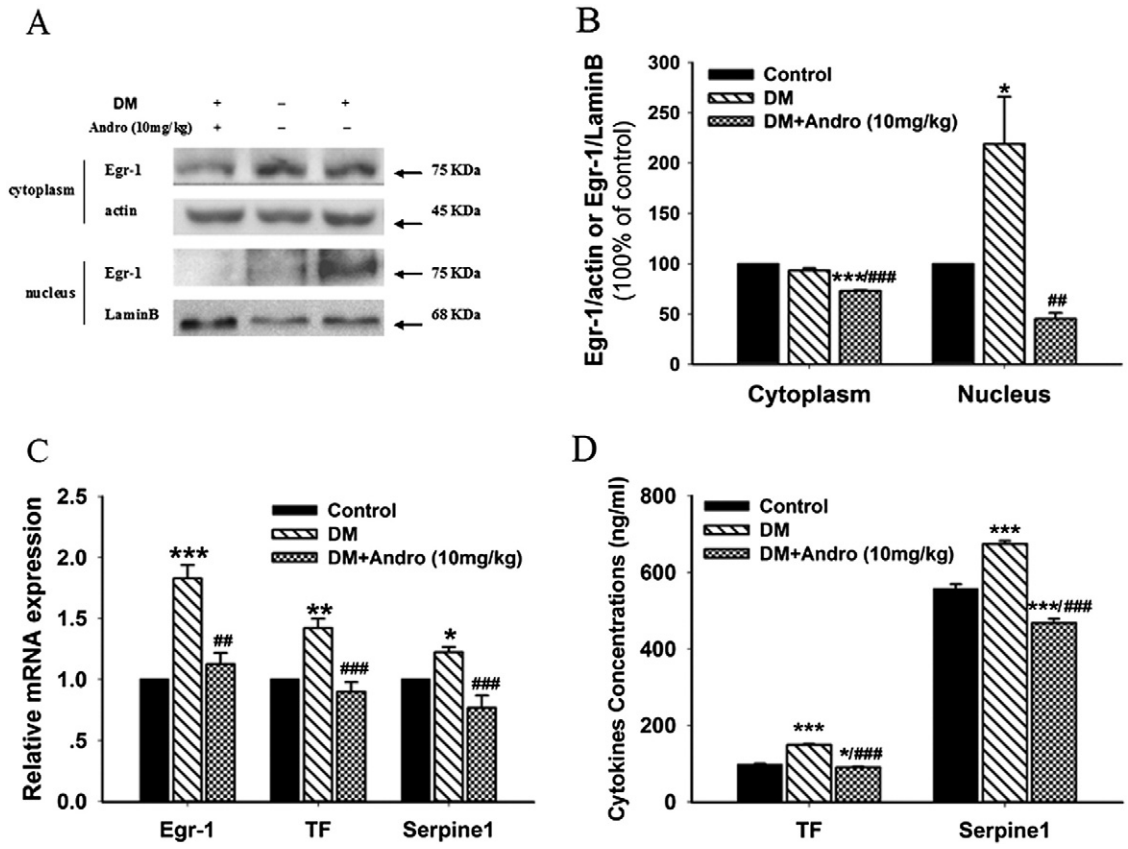

Fig. 5. Effect of Andro on Egr1 signaling pathway in STZ-induced NPDR mice. (A) Andro inhibited the nuclear translocation of Egr1 protein in retinas. Results represent at least three repeated experiments. (B) Quantitative densitometric analysis of Egr1 in cytoplasm and nucleus. (C) Retinal mRNA expression of Egr1, serpine1, TF. (D) Serum contents of serpine1 and TF. Data are expressed as means ± SEM (n = 9 for control, n = 11 for DM, n = 10 for Andro). $^{*}P < 0.05$, $^{**}P < 0.01$, $^{***}P < 0.001$ compared to control; $^{\#\#}P < 0.01$, $^{\#\#\#}P < 0.001$ compared to DM without Andro.

treated with Andro (10 mg/kg), the increased retinal nuclear Egr1 was obviously decreased in diabetic mice ($P < 0.01$). Andro (10 mg/kg) also weakly decreased the expression of Egr1 in retinal cytoplasm in diabetic mice ($P < 0.001$).

As shown in Fig. 5C, retinal mRNA expression of Egr1, TF and serpine1 was increased in STZ-induced diabetic mice ($P < 0.05$, $P < 0.01$, $P < 0.001$), whereas such increased mRNA expression was reduced in Andro-treated diabetic mice ($P < 0.01$, $P < 0.001$). In addition, the results of Fig. 5D showed that serum levels of TF and serpine1 were increased in STZ-induced diabetic mice ($P < 0.001$). After mice were treated with Andro (10 mg/kg), the elevated serum levels of TF and serpine1 were both decreased in diabetic mice ($P < 0.001$).

4. Discussion

Retinal neoangiogenesis is characterized by the growth of abnormal retinal vessels, which is the critical pathological changes during the development of DR, and it is also the hallmark of PDR [7]. The anti-angiogenic agents are considered as the promising treatment for DR [20,21]. Previous studies have showed the anti-angiogenic activity of Andro and its potential application in tumor growth inhibition [14–16]. Our present results showed that Andro reduced the increased number of retinal vessels in STZ-induced diabetic mice. This study is the first report about the inhibition of Andro on retinal angiogenesis during the development of PDR, which indicates the potential great value for the development of Andro for the treatment of DR.

VEGF, a well-known pro-angiogenic factor, plays important roles in regulating retinal angiogenesis [22,23]. Anti-VEGF therapy is considered as the feasible treatment for DR [24], and currently there are some anti-VEGF drugs including macugen (Pegaptanib sodium), lucentis (Ranibizumab), and avastin (Bevacizumab) under investigation to treat DR [25]. In the present study, we found that the elevated contents of VEGF in serum or vitreous cavity in STZ-induced PDR mice were both reduced after mice were treated with Andro. VEGF exerts its biological activity mainly via binding with its receptors like KDR or FLT1 [26]. Further results demonstrated that Andro decreased the increased retinal mRNA expression of VEGF and its two receptors including FLT1 and KDR. Our results indicate that Andro inhibits retinal angiogenesis via inhibiting VEGF signaling pathway, and thus contributes to the amelioration of PDR.

Retinal inflammation has also been reported to be critically involved in the development of DR, and specially NPDR [27]. The increased secretion of pro-inflammatory cytokines like TNF-α, IL-1β, and IL-6 will lead to the increased leukostasis and further breakdown of BRB during the development of NPDR [27,28]. NF-κB is a critical transcriptional factor involved in regulating inflammation [29]. NF-κB is responsible for inducing the production of various pro-inflammatory cytokines such as TNF-α and IL-1β [29,30]. Our results showed that Andro attenuated the increased BRB breakdown and reduced the elevated production of pro-inflammatory cytokines in STZ-induced NPDR mice. In addition, Andro decreased the increased nuclear translocation of NF-κBp65 and the phosphorylation of NF-κBp65, IκB, and IKK. All those results indicate that Andro can inhibit the activation of NF-κB signaling pathway, which contributes to the attenuation of retinal inflammation in STZ-induced NPDR mice and is helpful for the amelioration of NPDR.

Egr1 is another important transcriptional factor, and its main biological function is to transmit the signals involved in cell growth, differentiation, and apoptosis [31,32]. Egr1 is reported to be critically involved in various diseases such as tumor growth, and some cardiovascular pathological processes including ischemia and atherosclerosis [32–35].

Recently, there is a report that demonstrates that the high-mobility group box-1 (HMGB1)/receptor for advanced glycation end products (RAGE)/osteopontin (OPN)/early growth response-1 (Egr-1) pathway is involved in inflammatory, angiogenic, and fibrotic responses in proliferative vitreoretinal disorders including PDR [36]. In our present study, we found that Andro decreased the increased nuclear translocation of Egr1 in STZ-induced NPDR mice. The results clearly demonstrate the inhibition of Andro on the transcriptional activation of Egr1 in diabetic mice. Next, the results showed that Andro decreased the increased mRNA expression and serum contents of serpine1 and TF, which are both downstream genes regulated by Egr1 [37]. Serpine1, also named plasminogen activator inhibitor 1, is a rapid inhibitor of tissue plasminogen (tPA) and acts as the primary regulator of fibrinolysis, which is critically involved in modulating extracellular matrix proteolysis [38]. Recent studies demonstrate that the increased plasma serpine1 content is associated with the progression of DR [39,40]. TF, a transmembrane glycoprotein, is involved in regulating blood coagulation, and recent reports demonstrate its potential regulation of angiogenesis [41,42]. TF is also reported to be increased during the development of DR [43]. Thus, Andro-induced reduced expression of serpine1 and TF will be helpful for the amelioration of DR. Egr1 also contributes to the regulation of the production of some pro-inflammatory cytokines such as TNF-α and IL-6 [37,44]. Thus, Andro-induced decreased activation of Egr1 may also contribute to the reduced production of pro-inflammatory cytokines including TNF-α, IL-1β, and IL-6. All those results indicate that Andro-induced inhibition on Egr1 signaling pathway contributes to the amelioration of Andro on retinal inflammation or angiogenesis during the progression of DR.

In conclusion, our study demonstrates the obvious amelioration of Andro on retinal inflammation and angiogenesis during the development of DR, and VEGF, NF-κB, and Egr1 signals all play important roles in such process. This study provides the strong evidences for the potential application of Andro for the treatment of DR in clinic.

Conflict of interest

The authors declare no conflict of interest.

Acknowledgement

This work was financially supported by National Natural Science Foundation of China (81322053, 81173517), and Training Plan of Excellent Young Medical Talents in Shanghai (XYQ2011057).

References

[1] J.C. Chan, N.H. Cho, N. Tajima, J. Shaw, Diabetes in the Western Pacific Region—past, present and future, Diabetes Res. Clin. Pract. 103 (2014) 244–255.
[2] A. Willard, I.M. Herman, Vascular complications and diabetes: current therapies and future challenges, J. Ophthalmol. 2012 (2012) 209538.
[3] R.J. Fantes, V.D. Durairaj, S.C. Oliver, Diabetic retinopathy: an update on treatment, Am. J. Med. 123 (2010) 213–216.
[4] A.M. Abu El-Asrar, Evolving strategies in the management of diabetic retinopathy, Middle East Afr. J. Ophthalmol. 20 (2013) 273–282.
[5] R. Chibber, B.M. Ben-Mahmud, S. Chibber, E.M. Kohner, Leukocytes in diabetic retinopathy, Curr. Diabetes Rev. 3 (2007) 3–14.
[6] C.P. Wilkinson, F.L. Ferris III, R.E. Klein, P.P. Lee, C.D. Agardh, M. Davis, D. Dills, A. Kampik, R. Pararajaseqaram, J.T. Verdaquer, Global Diabetic Retinopathy Project Group, Proposed international clinical diabetic retinopathy and diabetic macular edema disease severity scales, Ophthalmology 110 (2003) 1677–1682.
[7] N. Cheung, P. Mitchell, T.Y. Wong, Diabetic retinopathy, Lancet 376 (2010) 124–136.
[8] D. Gologorsky, A. Thanos, D. Vavvas, Therapeutic interventions against inflammatory and angiogenic mediators in proliferative diabetic retinopathy, Mediat. Inflamm. 2012 (2012) 629452.
[9] J.C. Lim, T.K. Chan, D.S. Ng, S.R. Sagineedu, J. Stanslas, W.S. Wong, Andrographolide and its analogues: versatile bioactive molecules for combating inflammation and cancer, Clin. Exp. Pharmacol. Physiol. 39 (2012) 300–310.
[10] J. Li, L. Luo, X. Wang, B. Liao, G. Li, Inhibition of NF-kappaB expression and allergen-induced airway inflammation in a mouse allergic asthma model by andrographolide, Cell. Mol. Immunol. 6 (2009) 381–385.
[11] S.P. Guan, W. Tee, D.S. Ng, T.K. Chan, H.Y. Peh, W.E. Ho, C. Cheng, J.C. Mak, W.S. Wong, Andrographolide protects against cigarette smoke-induced oxidative lung injury via augmentation of Nrf2 activity, Br. J. Pharmacol. 168 (2013) 1707–1718.
[12] T. Zhu, W. Zhang, M. Xiao, H. Chen, H. Jin, Protective role of andrographolide in bleomycin-induced pulmonary fibrosis in mice, Int. J. Mol. Sci. 14 (2013) 23581–23596.
[13] W. Liu, W. Guo, L. Guo, Y. Gu, P. Cai, N. Xie, X. Yang, Y. Shu, X. Wu, Y. Sun, Q. Xu, Andrographolide sulfonate ameliorates experimental colitis in mice by inhibiting Th1/Th17 response, Int. Immunopharmacol. 20 (2014) 337–345.
[14] K. Sheeja, C. Guruvayoorappan, G. Kuttan, Antiangiogenic activity of andrographis paniculata extract and andrographolide, Int. Immunopharmacol. 7 (2007) 211–221.
[15] H.H. Lin, C.W. Tsai, F.P. Chou, C.J. Wang, S.W. Hsuan, C.K. Wang, J.H. Chen, Andrographolide down-regulates hypoxia-inducible factor-1α in human non-small cell lung cancer A549 cells, Toxicol. Appl. Pharmacol. 250 (2011) 336–345.
[16] K.K. Shen, L.L. Ji, B. Lu, C. Xu, C.Y. Gong, G. Morahan, Z.T. Wang, Andrographolide inhibits tumor angiogenesis via blocking VEGF/VEGFR2-MAPKs signaling cascade, Chem. Biol. Interact. 218 (2014) 99–106.
[17] C.Y. Gong, Z.Y. Yu, B. Lu, L. Yang, Y.C. Sheng, Y.M. Fan, L.L. Ji, Z.T. Wang, Ethanol extract of *Dendrobium chrysotoxum* Lindl ameliorates diabetic retinopathy and its mechanism, Vasc. Pharmacol. 62 (2014) 134–142.
[18] C.Y. Gong, B. Lu, Q.W. Hu, L.L. Ji, Streptozotocin induced diabetic retinopathy in rat and the expression of vascular endothelial growth factor and its receptor, Int. J. Ophthalmol. 6 (2013) 573–577.
[19] C.X. Huang, Experimental Study of Fufang XueshuanTong on Intervention of Retinopathy in Diabetic Rats, Sun Yat-Sen University, Guangzhou, 2006. 13–19 (In Chinese).
[20] V.S. Jeganathan, Anti-angiogenesis drugs in diabetic retinopathy, Curr. Pharm. Biotechnol. 12 (2011) 369–372.
[21] B. Kumar, S.K. Gupta, R. Saxena, S. Srivastava, Current trends in the pharmacotherapy of diabetic retinopathy, J. Postgrad. Med. 58 (2012) 132–139.
[22] N. Gupta, S. Mansoor, A. Sharma, A. Sapkal, J. Sheth, P. Falatoonzadeh, B. Kuppermann, M. Kenney, Diabetic retinopathy and VEGF, Open Ophthalmol. J. 7 (2013) 4–10.
[23] D.A. Antonetti, R. Klein, T.W. Gardner, Diabetic retinopathy, N. Engl. J. Med. 366 (2012) 1227–1239.
[24] P.M. Titchenell, D.A. Antonetti, Using the past to inform the future: anti-VEGF therapy as a road map to develop novel therapies for diabetic retinopathy, Diabetes 62 (2013) 1808–1815.
[25] G. Tremolada, C.D. Turco, R. Lattanzio, S. Maestroni, A. Maestroni, F. Bandello, G. Zerbini, The role of angiogenesis in the development of proliferative diabetic retinopathy: impact of intravitreal anti-VEGF treatment, Exp. Diabetes Res. 2012 (2012) 728325.
[26] J. Waltenberger, L. Claesson-Welsh, A. Siegbahn, M. Shibuya, C.H. Heldin, Different signal transduction properties of KDR and Flt1, two receptors for vascular endothelial growth factor, J. Biol. Chem. 269 (1994) 26988–26995.
[27] A.P. Adamis, Is diabetic retinopathy an inflammtory disease? Brit. J. Ophthalmol. 86 (2002) 363–365.
[28] E.C. Leal, J. Martins, P. Voabil, J. Liberal, C. Chiavaroli, J. Bauer, J. Cunha-Vaz, A.F. Ambrosio, Calcium dobesilate inhibits the alterations in tight junction proteins and leukocyte adhesion to retinal endothelial cells induced by diabetes, Diabetes 59 (2010) 2637–2645.
[29] P.A. Baeuerle, T. Henkel, Function and activation of NF-kappa B in the immune system, Annu. Rev. Immunol. 12 (1994) 141–179.
[30] P. Renard, M. Raes, The proinflammatory transcription factor NFkappaB: a potential target for novel therapeutical strategies, Cell Biol. Toxicol. 15 (1999) 341–344.
[31] A. Gashler, V. Sukhatme, Egr-1: prototype of a zinc finger family of transcription factors, Prog. Nucleic Acid Res. Mol. Biol. 50 (1995) 191–224.
[32] C. Liu, A. Calogero, G. Ragona, E. Adamson, D. Mercola, EGR-1, the reluctant suppression factor: EGR-1 is known to function in the regulation of growth, differentiation, and also has significant tumor suppressor activity and a mechanism involving the induction of TGF-beta1 is postulated to account for this suppressor activity, Crit. Rev. Oncog. 7 (1996) 1–2.
[33] E. Adamson, I. de belle, S. Mittal, Y. Wang, J. Hayakawa, K. Korkmaz, D. O'Hagan, M. McClelland, D. Mercola, Egr1 signaling in prostate cancer, Cancer Biol. Ther. 2 (2003) 617–622.
[34] L.M. Khachigian, Early growth response-1 in cardiovascular pathobiology, Circ. Res. 98 (2006) 186–191.
[35] S.F. Yan, E. Harja, M. Andrassy, F. Tomoyuki, A.M. Schmidt, Protein kinase C β/Early growth response-1 pathway: a key player in ischemia, atherosclerosis, and restenosis, J. Am. Coll. Cardiol. 48 (2006) A47–A55.
[36] A.M. El-Asrar, L. Missotten, K. Geboes, Expression of high-mobility groups box-1/receptor for advanced glycation and products/osteopontin/early growth response-1 pathway in proliferative vitreoretinal epiretinal membranes, Mol. Vis. 17 (2011) 508–518.
[37] A. Aljada, H. Ghanim, P. Mohanty, N. Kapur, P. Dandona, Insulin inhibits the pro-inflammatory transcription factor early growth response gene-1 (Egr)-1 expression in mononuclear cells (MNC) and reduces plasma tissue factor (TF) and plasminogen activator inhibitor-1 (PAI-1) concentrations, J. Clin. Endocrinol. Metab. 87 (2002) 1419–1422.
[38] P. Carmeliet, J.M. Stassen, L. Schoonjans, B. Ream, J.J. van den Oord, M. De Mol, R.C. Mulligan, D. Collen, Plasminogen activator inhibitor-1 gene-deficient mice. II. Effects on hemostasis, thrombosis, and thrombolysis, J. Clin. Invest. 92 (1993) 2756–2760.
[39] Z.L. Zhong, S. Chen, Plasma plasminogen activator inhibitor-1 is associated with end-stage proliferative diabetic retinopathy in the northern Chinese Han population, Exp. Diabetes Res. 2012 (2012) 350852.

[40] M.B. Grant, E.A. Ellis, S. Caballero, R.N. Mames, Plasminogen activator inhibitor-1 overexpression in nonproliferative diabetic retinopathy, Exp. Eye Res. 63 (1996) 233–244.
[41] P.M. Fernandez, F.R. Rickles, Tissue factor and angiogenesis in cancer, Curr. Opin. Hematol. 9 (2002) 401–406.
[42] R.S. Kasthuri, M.B. Taubman, N. Mackman, Role of tissue factor in cancer, J. Clin. Oncol. 27 (2009) 4834–4838.
[43] T. Sakamoto, S. Ito, H. Yoshikawa, Y. Hata, T. Ishibashi, K. Sueishi, H. Inomata, Tissue factor increases in the aqueous humor of proliferative diabetic retinopathy, Graefes Arch. Clin. Exp. Ophthalmol. 239 (2001) 865–871.
[44] J. Zhang, S. Xie, W. Ma, Y. Teng, Y. Tian, X. Huang, Y. Zhang, A newly identified microRNA, mmu-miR-7578, functions as a negative regulator in inflammatory cytokines tumor necrosis factor-α and interleukin-6 via targeting Egr1 *in vivo*, J. Biol. Chem. 288 (2013) 4310–4320.